

S. Bolegenova¹ , A. Askarova¹ , Sh. Ospanova^{2*} , N. Pilipenko³ ,
Zh. Shortanbayeva² , A. Aldiyarova² 

¹Institute of Experimental and Theoretical Physics, Kazakhstan, Almaty

²Al-Farabi Kazakh National University, Kazakhstan, Almaty

³ITMO University, Russian Federation, Saint Petersburg

*email: Shynar.Ospanova@kaznu.kz

SIMULATION OF ATOMIZATION AND IGNITION OF HIGH-PRESSURE JET STREAM

This work is a significant study in terms of modern combustion physics of the problem of computer modeling of atomization, ignition, and combustion of high-pressure reactive liquid fuels under high turbulence. The need for a detailed study of the physical and chemical processes occurring during the combustion of reactive fuels is determined by the increased requirements for the efficiency of various technical devices, the accuracy of ignition prediction, and the combustion rate conditioned by the current environmental requirements for environmental protection.

The processes of atomization, ignition, and combustion of atomized jet fuel (heptane) at high pressures were investigated using a numerical model. Numerical simulation methods were used to get profiles of the temperature plume, distribution of concentrations of the oxidizer, and reaction products (carbon dioxide and soot) in the combustion space. The optimum value of the initial pressure for heptane has been determined. The practical significance of the computational experiments presented in this paper is that the results obtained can be used in designing various reactive technical devices using combustion, which would simultaneously solve the problem of optimizing the process, increasing fuel combustion efficiency, and minimizing emissions of harmful substances.

Keywords: pressure, fuel jet, combustion, atomization, ignition, simulation.

С. Бөлегенова¹, Ә. Асқарова¹, Ш. Оспанова^{2*}, Н. Пилипенко³,
Ж. Шортанбаева², А. Алдиярова²

¹Эксперименттік және теориялық физика ғылыми-зерттеу институты, Қазақстан, Алматы қ.

²Әл-Фараби атындағы Қазақ ұлттық университеті, Қазақстан, Алматы қ.

³АТМО университеті, Ресей Федерациясы, Санкт-Петербург қ.

*email: Shynar.Ospanova@kaznu.kz

Жоғары қысымды реактивті ағыншаның бүрку және тұтануын модельдеу

Аталған жұмыс заманауи жану физикасы көзқарасы тұрғысынан жоғары турбуленттіліктегі жоғары қысымды реактивті сұйық отынның бүрку, тұтану және жануын компьютерлік модельдеу мәселесіне бағытталады. Әсерлесетін отындардың жануы барысында өтетін физика-химиялық процестерді мұқият зерттеудің қажеттілігі түрлі техникалық құрылғылардың жұмыс тиімділігіне қойылатын талаптардың артуымен, тұтануды болжау дәлдігімен, жану жылдамдығымен негізделеді және қоршаған ортаны қорғау бойынша заманауи экологиялық талаптармен анықталады.

Сандық модельдің көмегімен жоғары қысымда бүркілген реактивті отынның (гептан) бүрку, тұтану және жану процестері зерттелінді. Сандық модельдеу әдістері арқылы температуралық алау профильдері, тотықтырғыш пен жану өнімдерінің () концентрацияларының жану кеңістігінде таралуы анықталды. Гептан үшін бастапқы қысымның тиімді мәні анықталды. Аталған жұмыста келтірілген есептеуіш тәжірибелердің практикалық құндылығы алынған нәтижелердің жануға негізделген түрлі реактивті техникалық құрылғыларды жобалауда қолданылатындығымен анықталады. Олар бізмезгілде процесті оңтайландыру, отынның жану тиімділігін арттыру және зиянды заттардың шығынын азайту сияқты мәселелерді шешуге мүмкіндік береді.

Түйін сөздер: қысым, реактивті отын, жану, бүрку, тұтану, модельдеу.

С. Болегенова¹, А. Аскарлова¹, Ш. Оспанова^{2*}, Н. Пилипенко³,
Ж. Шортанбаева², А. Алдиярова²

¹Научно-исследовательский институт экспериментальной и теоретической физики, Казахстан, г.Алматы

²Казахский национальный университет им. аль-Фараби, Казахстан, г.Алматы

³Университет ИТМО, Российская Федерация, г.Санкт-Петербург

*email: Shynar.Ospanova@kaznu.kz

Моделирование распыла и воспламенения реактивной струи высокого давления

Данная работа посвящена важному исследованию с точки зрения современной физики горения проблемы компьютерного моделирования распыла, воспламенения и горения реактивного жидкого топлива высокого давления при высокой турбулентности. Необходимость детального исследования физико-химических процессов, протекающих при горении реагирующих топлив, определена возросшими требованиями к эффективности работы различных технических устройств, точности прогнозирования воспламенения, скорости горения и обусловлена современными экологическими требованиями по охране окружающей среды.

При помощи численной модели исследованы процессы распыла, воспламенения и горения распыленного реактивного топлива (гептан) при высоких давлениях. Методами численного моделирования получены профили температурного факела, распределения концентраций окислителя и продуктов реакций (двуокись углерода и сажа) в пространстве горения. Определено оптимальное значение начального давления для гептана. Практическая значимость вычислительных экспериментов, представленных в данной работе, состоит в том, что полученные результаты могут быть использованы при проектировании различных реактивных технических устройств, использующих горение, которые решали бы одновременно проблему оптимизации процесса, увеличения эффективности сгорания топлива и минимизации выбросов вредных веществ.

Ключевые слова: давление, реактивное топливо, горение, распыл, воспламенение, моделирование.

Introduction

The space sector of the global economy currently demonstrates dynamic and stable development due to the transfer of space technologies from the military sphere to the civil sphere and the development of a whole range of commercial services related to the space industry and developments. All in all, this contributes to the commercialization of space activities and rapid growth of the space industry, development, and sales of space products, technologies, and services, which, in turn, gives a major thrust to increasing industry competition at different levels: global, interregional, interstate and national.

In turn, the global space market is a large and rapidly developing segment of the global market of high technology. Innovative technologies in microelectronics, digital and information systems, software, communications, telecommunications, new composite materials, etc. are known to be one of the key drivers of modern economic progress. Most of these developments originate in various spheres of the space industry and significantly impact the most diverse areas of modern life.

According to the 2007 Euro consult analytical report, 79 states were involved in space activities to a

greater or lesser extent. Of this number, 30 states stand out, which actively and purposefully develop their national space (civil and military) programs, have their spacecraft, provide certain space services commercially, and actively take part in international space projects. These states are a group of highly competitive space market players [1, 2].

Due to the global pandemic in 2020, the growth in energy consumption in the world decreased by 4%. For comparison, in the period from 2000 to 2018, the average annual rate was 2%, and in 2019 it fell to 0.8%. Energy consumption has decreased in most countries. The exception is China (24% of international energy consumption in 2020), the largest consumer of energy and quickly recovered from the COVID-19 crisis. Energy consumption in China increased by 2.2%, which is much less than in previous years. In 2020, isolation measures were taken, and economic activity decreased, which significantly affected energy consumption. It declined strongly in the US (-7.6%), declined by about 7% in the EU (the strongest declines occurred in large markets such as Spain, France, Italy, and Germany), Japan, and Canada, and also fell by 4.8% in Russia (Figures 1 and 2) [3-6].

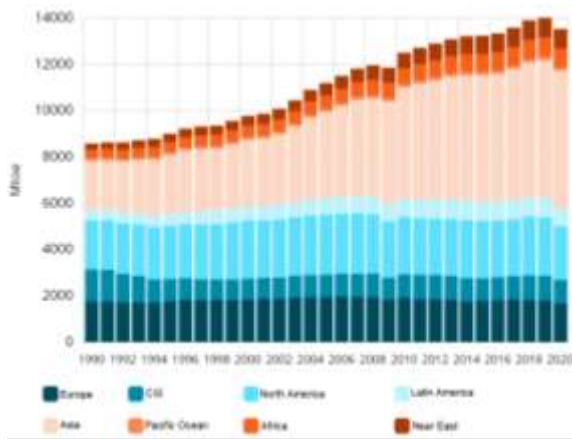


Figure 1 - Energy consumption trend for the period 1990 – 2020 [3]

The distinctive feature of the Asian market is the high degree of commercialization and integration of space services into the economic system. According to expert estimates, the Asian market has long-term growth potential and is, along with the North American market, one of the most promising and capacious for the next 10-15 years. Asia is going through a phase of the technological economy, and the presence of a powerful scientific and technical base (Japan, China, South Korea, Taiwan) and significant financial opportunities stimulate the development of the space technology market.

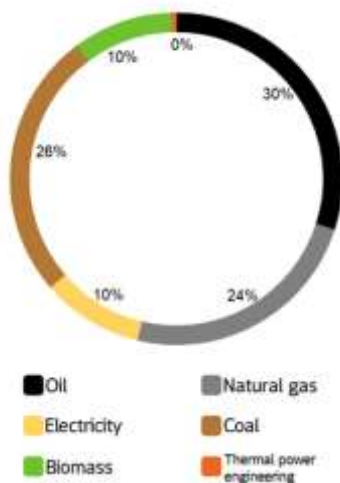


Figure 2 - Energy consumption by type for 2020 [3]

The Asian market demonstrates a steady increase in competition in the field of rocket and satellite construction and launch services, which, in turn, affects the global conjuncture: competition develops at the intra-regional and international levels. A great commercial interest in Asia is observed on the part of all major space equipment manufacturers and operators of space services. Today our republic aspires to take its place among the space powers of

the world. International procedures are currently underway for Kazakhstan to join the Missile Technology Control Regime, which will allow it to become a full-fledged participant in international space activities.

In recent years, the global space industry has undergone major changes related to the growing scale of international cooperation in space exploration and use, rapid globalization, and the commercialization of space activities. Many countries, including Kazakhstan, have come to understand the importance of their geopolitical interests in space, and as a result, space exploration and utilization have become a priority of national policy.

Under the approved State Program for the development of space activities, a joint Russian-Kazakh space project entitled «Baiterek» is being implemented for the construction of a space rocket complex with high environmental safety and environmental protection requirements.

Because of this investment project, Kazakhstan will have favorable opportunities to develop its national aerospace industry and space program, operate advanced, environmentally safe rocket and space equipment, meet all international standards, and create new jobs.

The national company «Kazkosmos» works actively; it has nine space projects in its arsenal, one of which, a special design office for space equipment, to be jointly established with the Russian space corporation «Energia», will be implemented at the cosmodrome.

The Astrophysical Research Center has got certain results in implementing scientific research in the space sphere. This applies to research work on participation in creating an international system for radiation monitoring of outer space, drafting a comprehensive program of scientific research and experiments of Kazakhstan on board the International Space Station, comprehensive studies of optical phenomena in the upper atmosphere, and other studies. In this way, space research and utilization play an ever-increasing role in the economic, scientific, technical, and social development of our State.

A turbojet engine gets the oxygen necessary for fuel combustion from the surrounding air, while a rocket engine carries the oxygen supply along with the fuel and is therefore not dependent on the presence of an atmosphere. Rocket engines can be divided into two dominant classes: two-component fuel engines, in which the fuel and oxidizer are placed in different tanks and injected in a certain proportion into the combustion chamber; single-component fuel engines, in which the fuel and oxidizer are in a bound state [7-10].

A wide variety of fuels can be used in liquid propellant rocket engines. The choice of fuel combination depends on the general data characterizing the engine: its purpose, power, and duration of operation. When choosing a fuel, it is necessary to evaluate the following properties: ignition rate, combustion rate, stability of components, density, volatility, specific heat capacity in the liquid state, corrosiveness, toxicity, freezing point, viscosity, and availability of sufficient stocks and cost. Fuels with a lower average molecular weight of the combustion products have the greatest practical value because such fuels require lower temperatures in the combustion chamber for a specific thrust than do fuels with a higher average molecular weight of the combustion products. Hence, fuels with a relatively high percentage of hydrogen are of most interest - especially such widely used hydrocarbons as gasoline, kerosene, diesel fuel, methyl, and ethyl alcohols [11-13].

The key factors determining a good engine design are good mixing and atomization of fuel components by nozzles; small internal surface area of the combustion chamber walls, not allowing much heat transfer; completeness of combustion mixture provided by the proper combustion chamber volume; strength of the chamber body; good streamlined internal chamber surface in order to avoid local overheating and related burn-out of chamber walls; small engine weight and ease of manufacturing.

The combustion process can be divided into several successive stages: the atomization of fuel components and their mixing, heating the mixture to ignition temperature, and combustion. These processes overlap to a greater or lesser extent depending on the engine design, for instance, atomization can be accompanied by mixing, heating, and even partial combustion. The combustion reaction proceeds faster if the components are in a gaseous state, so it is necessary to mix the fuel as thoroughly as possible and to make it gaseous before ignition.

Nozzles have for the most part been created empirically, so many different types of nozzles have been developed. The best-known of these is the vortex nozzle. The liquid enters the swirl nozzle chamber tangentially to its inner surface. The resulting swirl produces a very fine rotating cone as the fluid enters the combustion chamber. In many types of injection devices, the fuel components are injected through a large number of orifices to ensure uniform mixing. The high-temperature regime and continuous heat inflow create more stressful operating conditions for a rocket engine than for any other heat engine. The temperature in the combustion

chamber of most existing rocket engines ranges from 1500 to 2500°C.

In this paper, a straight-flow rocket engine was considered, which is an open cylinder with fuel injected inside. The mixture of air and fuel in this technique is ignited and burns continuously while the airflow passes through the combustion chamber. The gases flow out through the exhaust port at a much higher velocity than the airflow rate entering the air intake. This difference in velocity is what gives rise to the engine's thrust. The straight jet engine in its pure form becomes practically applicable already at high subsonic speeds, but the maximum efficiency is achieved at Mach numbers equal to 2.5-3.0 when its weight consumption is about six times less than the fuel consumption equal in a thrust rocket engine.

One of the important units of a direct-flow engine is the automatic fuel regulator. It performs three different functions: it regulates the fuel supply according to the flight speed; it automatically doses the fuel supply according to the flight altitude; the fuel regulator is supposed to prevent the engine from stalling if the projectile in controlled flight assumes such large angles of attack that it might affect the operation of the air intake.

Mathematical model and methods

In this work method of floating stochastic particles was used. This method of simulation of the liquid core simulation was proposed in [14].

This method is based on the following assumptions:

1. At each time, simultaneously with the computation of flow in the gas, the liquid non-depleted jet has a random geometrical configuration. Each geometrical configuration is determined by the spatial trajectory of specific floating stochastic particles with zero masse.

2. At different times, the random configurations of liquid non-depleted jet represent an ensemble of independent realizations in space. The floating stochastic particles are injected one after another; each particle proceeds its own path, which ends up after a length of time referred to as the lifetime of the particle. The last one is determined from the dimension analyses. It is assumed that the overall time of the primary air-blast atomization is controlled by three physical values.

3. In the downstream direction, each stochastic particle is moving with a constant axial velocity equal to the convection velocity.

4. During the particle motion, each position indicates the cell containing the instantaneous interface, separating the liquid non-depleted domain from the gas (Figure 3).

5. The spray around the non-depleted liquid core is assumed to be thin (the droplet around are assumed to be negligible volume but with significant mass in comparison to the gas).

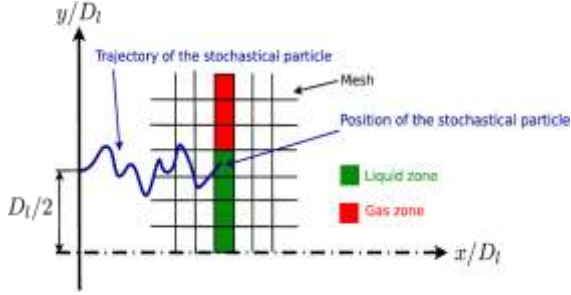


Figure 3 - Schematic of simulation of the liquid core configuration [14, 15]

In computational fluid dynamics, the immersed boundary method originally referred to an approach developed by Charles Peskin in 1972 to simulate fluid-structure interactions [16]. Treating the coupling of the structure deformations and the fluid flow poses a number of challenging problems for numerical simulations (the elastic boundary changes the flow of the fluid and the fluid moves the elastic boundary simultaneously). In the immersed boundary method the fluid is represented on an Eulerian coordinate and the structure is represented on a Lagrangian coordinate (Figure 4).

The basic equations of the mathematical model of the problem of atomization and combustion of liquid fuel are represented by the equations of continuity, motion, internal energy, k-ε model of turbulence [17-20].

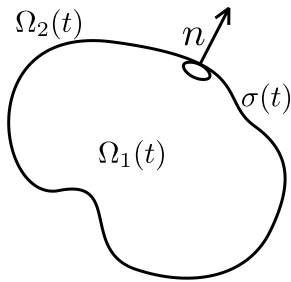


Figure 4 - Fluid domain separated by immersed massless boundary

The continuity equation for the reaction component m has the form [17, 19]:

$$\frac{\partial \rho_m}{\partial t} + \vec{\nabla}(\rho_m \vec{u}) = \vec{\nabla} \left[\rho D \vec{\nabla} \left(\frac{\rho_m}{\rho} \right) \right] + \dot{\rho}_m^c + \dot{\rho}_m^s \delta_{m1}, \quad (1)$$

where D is diffusion coefficient, $\vec{\nabla}$ is gradient operator, ρ_m is mass density of liquid phase, ρ is total

mass density, $\dot{\rho}_m^c$ is chemical source term; $\dot{\rho}^s$ is source term due to injection; u - velocity of the liquid.

Let us use Fick's law with the diffusion coefficient D . The component m_l is the component from which the injection droplets are formed, and δ is the Dirac delta function. Since mass is conserved in chemical reactions, summing equation (1) for all components we obtain the continuity equation for liquid, which has the form below [18]:

$$\frac{\partial \rho}{\partial t} + \vec{\nabla}(\rho \vec{u}) = \dot{\rho}^s. \quad (2)$$

Equation of motion for a mixture of liquids:

$$\frac{\partial(\rho \vec{u})}{\partial t} + \vec{\nabla}(\rho \vec{u} \vec{u}) = -\frac{1}{a^2} \vec{\nabla} p - A_0 \vec{\nabla} \left(\frac{2}{3} \rho k \right) + \vec{\nabla} \vec{\sigma} + \vec{F}^s + \rho \vec{g}, \quad (3)$$

where p is fluid pressure. The measureless value α is used in the PGS method. This is a method that improves computational efficiency in low Mach number flows where the pressure is approximately homogeneous. In equation (3), A_0 is 0 in the case of laminar flow and 1 when one of the turbulence models is used. The viscous stress tensor has the form [21]:

$$\sigma = \mu \left[\vec{\nabla} \vec{u} + (\vec{\nabla} \vec{u})^T \right] + \lambda \vec{\nabla} \vec{u} \vec{I}. \quad (4)$$

μ and λ are viscosity coefficients, and g is gravity acceleration.

The internal energy equation [22] is presented below:

$$\frac{\partial(\rho \vec{I})}{\partial t} + \vec{\nabla}(\rho \vec{u} \vec{I}) = -\rho \vec{\nabla} \vec{u} + (1 - A_0) \vec{\sigma} \vec{\nabla} \vec{u} - \vec{\nabla} \vec{J} + A_0 \rho \varepsilon + \dot{Q}^c + \dot{Q}^s, \quad (5)$$

where I is the specific internal energy, \dot{Q}^c is the source term due to heat release from the chemical reaction, and \dot{Q}^s is the heat brought by the injected fuel. The vector of heat change J is composed of the electric conductivity and enthalpy transfer:

$$\vec{J} = -K \vec{\nabla} T - \rho D \sum_m h_m \vec{\nabla} (\rho_m / \rho), \quad (6)$$

where T is liquid temperature, h_m is the enthalpy of component m . When one of the turbulence models is used ($A_0=1$), two equations are solved for the turbulence kinetic energy k and its dissipation rate ε [19, 20]:

$$\frac{\partial \rho k}{\partial t} + \vec{\nabla} \cdot (\rho \vec{u} k) = -\frac{2}{3} \rho k \vec{\nabla} \cdot \vec{u} + \sigma \cdot \nabla \vec{u} + \vec{\nabla} \cdot \left[\left(\left(\frac{\mu}{Pr_k} \right) \vec{\nabla} k \right) \right] - \rho \varepsilon + \dot{W}^s, \quad (7)$$

$$\frac{\partial \rho \varepsilon}{\partial t} + \vec{\nabla} \cdot (\rho \vec{u} \varepsilon) = -\left(\frac{2}{3} c_{\varepsilon 1} - c_{\varepsilon 2} \right) \rho \varepsilon \vec{\nabla} \cdot \vec{u} + \vec{\nabla} \cdot \left[\left(\left(\frac{\mu}{Pr_\varepsilon} \right) \vec{\nabla} \varepsilon \right) \right] + \frac{\varepsilon}{k} \left[c_{\varepsilon 1} \vec{\sigma} \vec{\nabla} \vec{u} - c_{\varepsilon 2} \rho \varepsilon + c_s \dot{W}^s \right]. \quad (8)$$

These are the standard k - ε equations. The expression $\left(\frac{2}{3} c_{\varepsilon 1} - c_{\varepsilon 2} \right) \vec{\nabla} \cdot \vec{u}$ in the ε -equation accounts for the length of the scale changes when there is velocity propagation. Initial conditions attract a value of \dot{W}^s , resulting from the interaction with the atomizer. The values of $c_{\varepsilon 1}$, $c_{\varepsilon 2}$, c_s , Pr_k , Pr_ε are constants that are determined from experiments and some theoretical considerations [17]. The value of $c_s = 1.50$ is proposed that it is based on the postulate of the length of scale conservation in the interaction of the turbulent jet and agrees well with the size of diesel jets.

In this paper, the atomization of fuel (heptane) in the combustion chamber at high turbulence and different pressure values is considered. A liquid fuel with a mass of 0.06 g at a temperature of 300 K is atomized through a nozzle in the center of the base of the combustion chamber. The optimal values of these physical quantities were taken from the previous works of the authors [6, 7, 20, 23].

The fuel injected into the combustion chamber, which is filled with air, undergoes a process of rapid evaporation, after which it burns in the gas phase. The process of liquid fuel combustion takes on average 4 ms. During the computational experiment, the pressure in the combustion chamber varied from 20 bar to 200 bar with an interval of 20 bar for heptane.

Heptane is used as rocket fuel and is a colorless, flammable liquid with a flash point of minus 4°C and an auto-ignition temperature of 223 °C. The inflammability range of heptane vapors in the air is 1.1-6.7% (by volume). Heptane belongs to hazard class 3. Heptane is a hydrocarbon of the paraffinic series.

Results and Discussion

This section presents the results of computer simulation of the atomization, ignition, and combustion of high-pressure jet fuel (heptane) in high turbulence. Computational experiments were performed depending on the initial pressure value from 20 to 200 bar.

Figure 5 shows the dependence of temperature on pressure for heptane. Looking at the figure, we can see that the maximum temperature of heptane droplets reaches 561 K at a pressure of 100 bar, and then it does not rise above this value when the pressure in the combustion chamber increases.

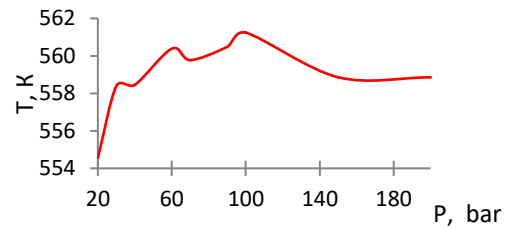


Figure 5 - Dependence of the temperature of liquid fuel droplets (heptane) on the pressure in the combustion chamber

Figure 6 contains a general picture of the effect of the pressure in the combustion chamber on the size of the atomization area. We see that for heptane, an increase in pressure in the combustion chamber from 20 bar to 200 bar leads to a decrease in the atomization area from 1.3 cm to 0.4 cm, i.e. the penetration height of droplets decreases.

The combustion mechanism of liquid fuels is characterized because the boiling point of liquid fuels is always below the autoignition temperature, so the combustion of liquid fuels occurs in the vapor phase.

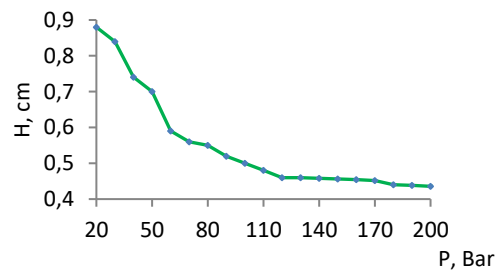


Figure 6 - Pressure dependence of the size of the heptane droplet spray area

The combustion mechanism of liquid fuels includes several stages: a spark (or other extraneous sources), ignition of the vapor-air mixture, combustion of the vapor-air mixture at the liquid surface, increase of the vaporization rate due to heat transfer from the flame (until equilibrium is reached). The ignition temperature of liquid fuel is considered

to be the heating temperature of the liquid fuel base, at which the fuel droplets ignite and a continuous process of fuel combustion occurs.

Figures 7-8 show the results of the investigation of the effect of pressure in the combustion chamber on the ignition and combustion processes of liquid fuel under high turbulence.

Analysis of Figure 7 shows that for heptane, a change in pressure from 40 to 60 bar leads to a quite obvious increase in the temperature in the combustion chamber, which lies between 741 K and 1923 K at 40 bar, and between 762 K and 1936 K at 60 bar. At the same time, an increase in pressure leads, for obvious reasons, to a decrease in the area occupied by fuel in the combustion chamber and to a delay in the ignition time from $t = 5.75 \cdot 10^{-4}$ s to $t = 5.82 \cdot 10^{-4}$ s.

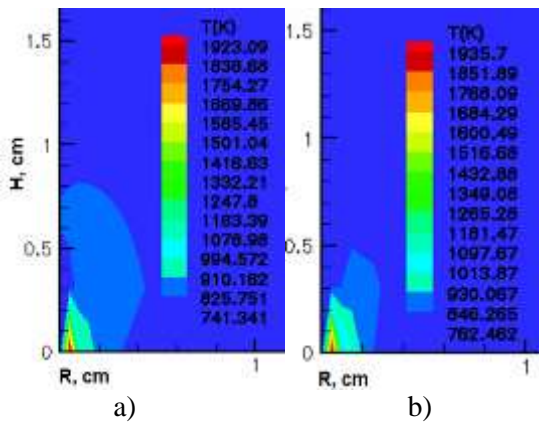


Figure 7 - Temperature distribution at the moment of heptane ignition at various pressures:
 a) $P = 40$ bar and $t = 5.75 \cdot 10^{-4}$ s,
 b) $P = 60$ bar and $t = 5.82 \cdot 10^{-4}$ s

A further increase in pressure leads to the fact that at a pressure of 100 bar, the area occupied by the fuel in the combustion chamber and the temperature are maximal. A further increase in pressure to 150 bar and higher reduces this area, as well as the temperature in the combustion chamber, slowing down the ignition process (Figure 8).

Figure 9 shows the results of a numerical simulation of the effect of pressure in the combustion chamber on the combustion process of liquid fuel (heptane).

Atomizing liquid fuel in a stationary or moving gas produces a two-phase reacting jet that burns to form a liquid fuel plume. As shown in Figure 9 (a, b) for heptane, an increase in pressure in the combustion chamber leads to an increase in the high-temperature region. This behavior can be observed up to a pressure of 100 bar for octane. A further increase in the pressure in the combustion chamber leads to a narrowing of the high-temperature range, and already at a pressure of 150 bar, this range decreases 9 (c).

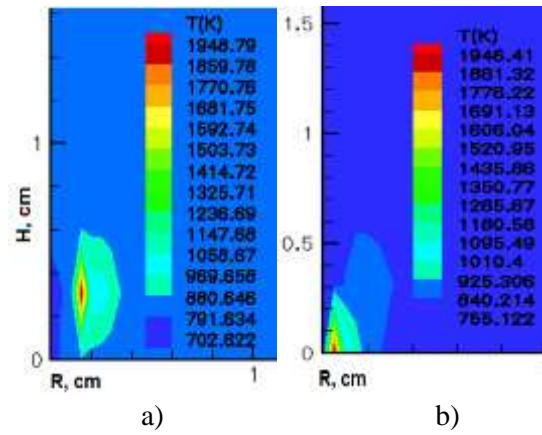


Figure 8 - Temperature distribution at the moment of heptane ignition at various pressures:
 a) $P = 100$ bar and $t = 7 \cdot 10^{-4}$ s,
 b) $P = 150$ bar and $t = 8 \cdot 10^{-4}$ s

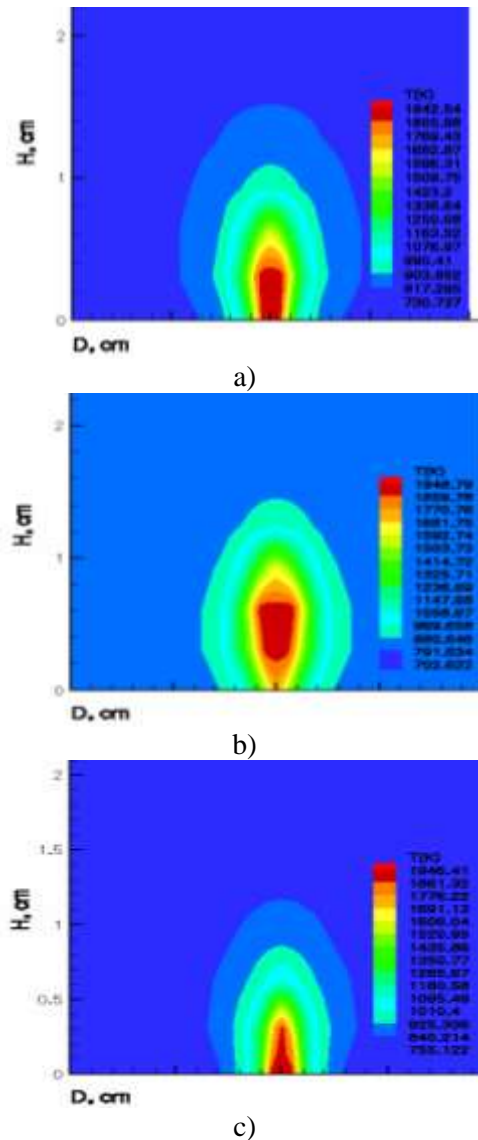


Figure 9 - Distribution of the maximum temperature of heptane at time $t = 1.5 \cdot 10^{-3}$ s at pressures:
 a) $P = 80$ bar, b) $P = 100$ bar and c) $P = 150$ bar

Analysis of Figure 10 for heptane shows that, as expected, with increasing pressure up to 100 bar, the area of maximum oxygen consumption decreases as the fuel concentration decreases. At a pressure in the combustion chamber of 150 bar, the fuel concentration increases slightly, so the area of maximum oxygen consumption decreases (Fig. 10 c).

The soot formation process is complex. Soot is an amorphous carbon residue produced by the incomplete combustion of fuel. The soot produced by internal combustion engines is emitted together with the products of combustion into the atmosphere as harmful fumes. Soot particles do not interact with air oxygen and are therefore removed only by coagulation and deposition.

The results of the computational experiment on the effect of pressure in the combustion chamber on the formation of soot and carbon dioxide during the combustion of heptane are shown in Figures 11 and 12. Analysis of Figure 11 shows that with increasing pressure, the area of maximum soot concentration decreases because, as the density of the oxidizer in the combustion chamber increases, the resistance exerted by the oxidizer on soot also increases.

Figure 12 shows the effect of the pressure in the combustion chamber on the distribution of carbon dioxide concentration. As the pressure increases from 40 bar to 100 bar, the maximum concentration of CO₂ decreases, as does the area of high concentrations of carbon dioxide.

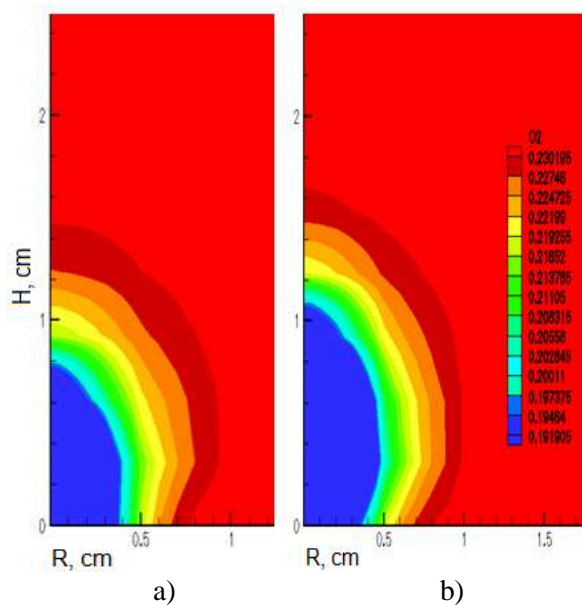


Figure 10 - The distribution of oxygen concentration during combustion of heptane at various pressures:
a) 100 bar, b) 150 bar at time $t = 1.5 \cdot 10^{-3}$ s

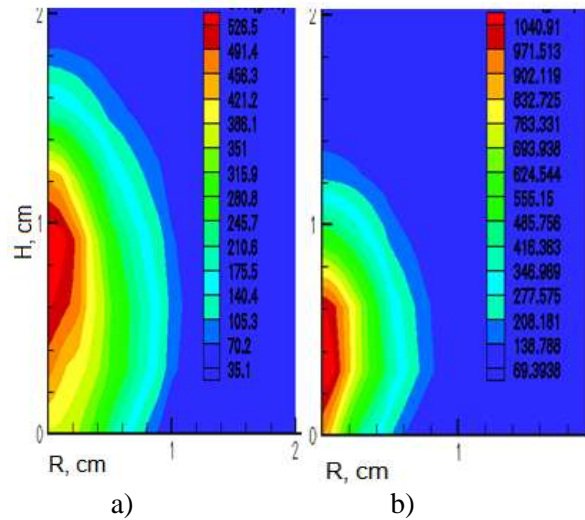


Figure 11 - Distribution of soot concentration during combustion of heptane at time $t = 1.5 \cdot 10^{-3}$ s at pressure:
a) 40 bar, b) 100 bar

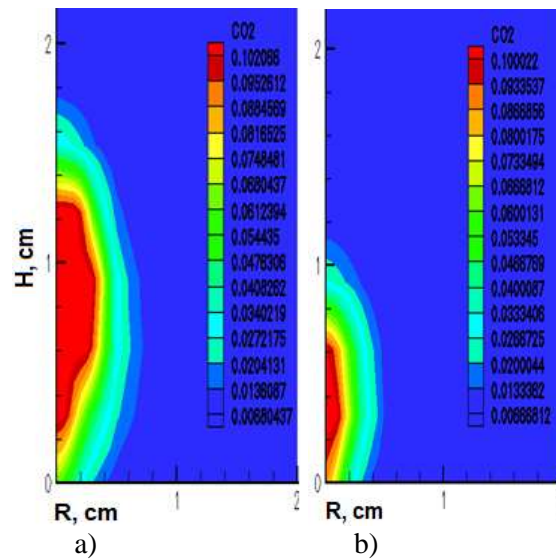


Figure 12 - Distribution of carbon dioxide concentration during combustion of heptane at time $t = 1.5 \cdot 10^{-3}$ s at pressure:
a) 40 bar, b) 100 bar

Conclusion

In this work, based on a numerical model of droplet atomization, computational experiments were performed to simulate the ignition and combustion of liquid fuel in the combustion chamber under high turbulence. Depending on different values of pressure in the combustion chamber, the temperature fields and distributions of the combustion products of heptane, which are most commonly used in rocket technology, were obtained.

When investigating the effect of the pressure in the combustion chamber from 20 to 200 bar at high turbulence on the particle temperature, it was determined that the droplet size for heptane practically did not change with increasing pressure in the combustion chamber. Regarding pressure, we determined that the optimal pressure for heptane is 100 bar. At this pressure, the droplet temperature reaches its maximum value. For heptane, it is 561 K. In this case, intensive evaporation of liquid fuel begins and the number of liquid droplets sharply decreases. A few of the smallest fuel droplets remain in the combustion chamber.

A study of the effect of pressure in the combustion chamber on ignition and combustion of liquid fuel at high turbulence showed that, for heptane, an increase in pressure in the combustion chamber leads to an increase in the region of high temperatures and a delay in the ignition time. This behavior can be observed up to a pressure of 100 bar. A further increase in the pressure in the combustion chamber causes the area of high temperatures to

narrow, and already at a pressure of 150 bar, this area decreases. With increasing pressure up to 100 bar, the area of maximum oxygen consumption decreases as the fuel concentration decreases. At a pressure in the combustion chamber of 150 bar, the fuel concentration increases slightly, so the area of maximum oxygen consumption decreases. The soot concentration increases significantly up to 10.41 g/m³, and the carbon dioxide concentration decreases.

The results can be used for the development of such fields of science as combustion physics, computational fluid dynamics, numerical methods in thermal physics and thermal power engineering, as well as in the design of new generation internal combustion engines.

Acknowledge

This work was supported by the Ministry of Education and Science of the Republic of Kazakhstan No. AP19679741.

References

- 1 Poinssot Ch., et al. Assessment of the environmental footprint of nuclear energy systems. Comparison between closed and open fuel cycles // *Energy*. – 2014. – Vol. 69. – P. 199-211.
- 2 Naser H. Analysing the long-run relationship among oil market, nuclear energy consumption, and economic growth: An evidence from emerging economies // *Energy*. – 2015. – Vol. 89. – P. 421-434.
- 3 Data of an independent information and consulting company Enerdata, 2021. <https://www.enerdata.net/>
- 4 Beketayeva M., Bolegenova S., et al. Computational method for investigation of solid fuel combustion in combustion chambers of a heat power plant // *High Temperature*. – 2015. – Vol. 53. – P. 751-757.
- 5 Askarova A., et al. Processes of heat and mass transfer in furnace chambers with combustion of thermochemically activated fuel // *Thermophysics and Aeromechanics*. – 2019. – Vol. 26. – P. 925-937.
- 6 Askarova A., et al. Investigation of the different Reynolds numbers influence on the atomization and combustion processes of liquid fuel // *Bulgarian Chemical Communications*. – 2018. – Vol. 50. – P. 68-77.
- 7 Mazhrenova N., et al. 3D modelling of heat and mass transfer processes during the combustion of liquid fuel // *Bulgarian Chemical Communications*. – 2016. – Vol. 48. – P. 229-235.
- 8 Askarova A., et al. On the effect of the temperature boundary conditions on the walls for the processes of heat and mass transfer // *International Journal of Mechanics*. – 2016. – Vol. 10. – P. 249-255.
- 9 Dubovas A., et al. Research on characteristics of turbo jet engine combustion chamber // *Aviation*. – 2021. – Vol. 25, Issue 1. – P. 65-72.
- 10 Shengxi J., et al. Dynamic characteristics analysis and optimization design of a simulated power turbine rotor based on finite element method // *International Journal of Turbo & Jet-Engines*. – 2017. – Vol. 37, Issue 1. – P. 31-39.
- 11 Wang H., et al. The effects of DI fuel properties on the combustion and emissions characteristics of RCCI combustion // *Fuel*. – 2018. – Vol. 227. – P. 457-468.
- 12 Fang W., et al. Optimization of reactivity-controlled compression ignition combustion fueled with diesel and hydrous ethanol using response surface methodology // *Fuel*. – 2015. – Vol. 160. – P. 446-457.
- 13 Safarik P., et al. Investigation of heat and mass transfer processes in the combustion chamber of industrial power plant boiler. Part 2. Distribution of concentrations of O₂, CO, CO₂, NO // *Journal of Applied and Computational Mechanics*. – 2018. – Vol. 12. – P. 127-138.
- 14 Gorokhovski M., et al. Stochastic model of the near-to-injector spray formation assisted by a high-speed coaxial gas jet // *Fluid Dynamics Research*. – 2009. – Vol. 41, Number 3. – P. 035509.

- 15 Gorokhovski M., et al. Stochastic scalar mixing models accounting for turbulent frequency multiscale fluctuations // *International journal of heat and fluid flow*. – 2004. – Vol. 25. – P. 875-883.
- 16 Peskin Ch. Flow patterns around heart valves: A numerical method // *Journal of Computational Physics*. – 1972. – Vol. 10, Issue 2. – P. 252-271.
- 17 Amsden A.A., O'Rourke P.J., Butler T.D. KIVA-II: A computer program for chemically reactive flows with sprays. - Los Alamos, 1989. – 160 p.
- 18 Ospanova Sh., Berezovskaya I., et al. Numerical simulation of the oxidant's temperature and influence on the liquid fuel combustion processes at high pressures // *Journal of Engineering and Applied Sciences*. – 2015. – Vol. 10. – P. 90-95.
- 19 Bolegenova S., Askarova A., et al. Investigation of the droplet dispersion influence on the atomization of liquid fuel processes in view of large-scale structures formation // *Recent Contributions to Physics*. – 2022. – Vol. 80, Issue 1. – P. 62-71.
- 20 Bolegenova S., Ospanova Sh., et al. Investigation of various types of liquid fuel atomization and combustion processes at high turbulence // *Journal of Engineering and Applied Sciences*. – 2018. – Vol. 13. – P. 4054-4064.
- 21 Apte S., et al. LES of atomizing spray with stochastic modeling of secondary break-up // *International Journal of Multiphase Flow*. - 2003. – Vol. 29, Issue 9. - P.1503–1522.
- 22 Bolegenova S., Messerle V., et al. Investigation of the liquid fuel single-hole injection in the combustion chamber // *Recent Contributions to Physics*. – 2020. – Vol. 75, Issue 4. – P. 62-71.
- 23 Bolegenova S., et al. Influence of boundary conditions to heat and mass transfer processes // *International Journal of Mechanics*. – 2016. – Vol. 10. – P. 320-325.

References

- 1 Ch. Poinssot, et al., *Energy*, 69, 199-211 (2014).
- 2 H. Naser, *Energy*, 89, 421-434 (2015).
- 3 Data of an independent information and consulting company Enerdata, 2021. <https://www.enerdata.net/>
- 4 M. Beketayeva, et al., *High Temp.*, 53, 751-757 (2015).
- 5 A. Askarova, et al., *Thermophys. Aeromechanics*, 26, 925-937 (2019).
- 6 A. Askarova, et al., *Bulg. Chem. Commun.*, 50, 68-77 (2018).
- 7 N. Mazhrenova, et al., *Bulg. Chem. Commun.*, 48, 229-235 (2016).
- 8 A. Askarova, et al., *Int. J. Mech.*, 10, 249-255 (2016).
- 9 A. Dubovas, et al., *Aviation*, 25, 65-72 (2021).
- 10 J. Shengxi, et al., *Int. J. Turbo Jet Engines*, 37, 31-39 (2017).
- 11 H. Wang, et al., *Fuel*, 227, 457-468 (2018).
- 12 W. Fang, et al., *Fuel*, 160, 446-457 (2015).
- 13 P. Safarik, et al., *J. Appl. Comput. Mech.*, 12, 127-138 (2018).
- 14 M. Gorokhovski, et al., *Fluid Dyn. Res.*, 41, 035509 (2009).
- 15 M. Gorokhovski, et al., *Int. J. Heat Fluid Flow*, 25, 875-883 (2004).
- 16 Ch. Peskin, et al., *J. Comput. Phys.*, 10, 252-271 (1972).
- 17 A.A. Amsden, et al., Los Alamos, 160 (1989).
- 18 Sh. Ospanova, et al., *J. Eng. Appl. Sci.*, 10, 90-95 (2015).
- 19 S. Bolegenova, et al., *Rec. Contr. Phys.*, 80, 62-71 (2022).
- 20 S. Bolegenova, et al., *J. Eng. Appl. Sci.*, 13, 4054-4064 (2018).
- 21 S. Apte, et al., *Int. J. Multiph. Flow*, 29, 1503–1522 (2003).
- 22 V. Messerle, et al., *Rec. Contr. Phys.*, 75, 62-71 (2020).
- 23 S. Bolegenova, et al., *Int. J. Mech.*, 10, 320-325 (2016).